Controlling the Optical Properties of Lemongrass Extract Synthesized Gold Nanotriangles and Potential Application in Infrared-Absorbing Optical Coatings

S. Shiv Shankar,[†] Akhilesh Rai,[†] Absar Ahmad,[‡] and Murali Sastry*[,†]

Nanoscience Group, Materials Chemistry Division and Biochemical Sciences Division, National Chemical Laboratory, Pune 411 008, India

Received September 29, 2004. Revised Manuscript Received November 23, 2004

Anisotropic metal nanoparticles have distinct optical behavior when compared with their spherical counterparts. In this report, we demonstrate a simple method involving the reduction of aqueous gold ions by the extract of the lemongrass plant leading to the formation of gold nanotriangles with interesting absorption in the near-infrared (NIR) region of the electromagnetic spectrum. We show that, by simple variation of the experimental conditions, it is possible to vary the size of the gold nanotriangles and, thus, to tune the absorbance of flat gold nanoparticles in the NIR region. The NIR absorption of the gold nanotriangles is expected to be of application in hyperthermia of cancer cells and in IR-absorbing optical coatings. We show that the lemongrass extract synthesized gold nanotriangles can be easily cast in the form of films on glass substrates and that these films are highly efficient in absorbing IR radiation for potential architectural applications.

Introduction

The biocompatibility of gold nanoparticles and the ease with which their surface may be functionalized using thiol and amine chemistry has led to many biomedical applications[1] apart from applications in catalysis[2] and sensors.[3] Spherical gold nanoparticles of diameters less than 20 nm absorb in the visible region of the electromagnetic spectrum (at ∼520 nm) due to excitation of surface plasmon vibrations (also known as the surface plasmon resonance or SPR) in the particles.[4] It is well known that open aggregated structures of gold nanoparticles and particles possessing an intrinsic anisotropy (for example, nanorods and nanotriangles) exhibit two prominent absorption bands, a low wavelength transverse absorption band (out-of-plane vibration band) and a longitudinal absorption band at longer wavelengths (in-plane plasmon vibrations).[5−7] In the former case, the additional long wavelength plasmon vibrations are due to interparticle plasmon coupling and linearly assembled superstructures of nanoparticles are currently being investigated for application in nanoscale optical waveguides.[8] In the case of anisotropic nanoparticles, the longitudinal plasmon absorption band is a strong function of the aspect ratio of the nanoparticle.[6] Under certain conditions of anisotropy, the longitudinal component of the SPR for nanorods can extend into near-infrared (NIR) region of the electromagnetic spectrum.[6c]

Though many synthesis protocols are available in the literature for the synthesis of gold nanoparticles with precise control of size and polydispersity,[9] relatively fewer reports are available for the synthesis of anisotropic metal nanoparticles. A large percentage of the reports have concentrated on the synthesis of gold nanorods[10] and only very recently have alternative structures such as nanotriangles been attempted.[11] In a preliminary report, we have recently reported on the synthesis of highly anisotropic gold nanotriangles using lemongrass extract as the reducing agent.[7] These nanotriangles possess a very broad in-plane SPR band that extends well into the NIR and exhibit considerable anisotropy in electronic conduction as well.[7] The NIR absorption of such gold nanostructures has many potential applications, one of the exciting ones being in hyperthermia of cancer cells.

* To whom correspondence should be addressed. E-mail: sastry@ems.ncl.res.in.

[†] Nanoscience Group, Materials Chemistry Division.

[‡] Biochemical Sciences Division.

(1) (a) Gu, H. Y.; Chen, Z.; Sa, R. X.; Yuan, S. S.; Chen, H. Y.; Ding, Y. T.; Yu, A. M. *Biomaterials* **2004**, *25*, 3445−3451. (b) Sandhu, K. K.; McIntosh, C. M.; Simard, J. M.; Smith, S. W.; Rotello, V. M. *Bioconjugate Chem.* **2002**, *13*, 3−6.

(2) Moreno-Manas, M.; Pleixats, R. *Acc. Chem. Res.* **2003**, *36*, 638−643.

(3) (a) Mirkin, C. A.; Letsinger, R. L.; Mucic, R. C.; Storhoff, J. J. *Nature* **1996**, *382*, 607−609. (b) Han, M.; Gao, X.; Su, J. Z.; Nie, S. *Nat. Biotechnol.* **2001**, *19*, 631−635.

(4) (a) Henglein, A. *J. Phys. Chem.* **1993**, *97*, 5457−5471. (b) Mulvaney, P. *Langmuir* **1996**, *12*, 788−800.

(5) Shipway, A. N.; Lahav, M.; Gabai, R.; Willner, I. *Langmuir* **2000**, *16*, 8789−8795.

(6) (a) Kelly, K. L.; Coronado, E.; Zhao, L. L.; Schatz, G. C. *J. Phys. Chem. B* **2003**, *107*, 668−677. (b) El-Sayed, M. A. *Acc. Chem. Res.* **2001**, *34*, 257−264. (c) Link, S.; Mohamed, M. B.; El-Sayed, M. A. *J. Phys. Chem. B* **1999**, *103*, 3073−3077.

(7) Shankar, S. S.; Rai, A.; Ankamwar, B.; Singh, A.; Ahmad, A.; Sastry, M. *Nat. Mater.* **2004**, *3*, 482−488.

(8) Maier, S. A.; Brongersma, M. L.; Kik, P. G.; Meltzer, S.; Requicha, A. A. G.; Atwater, H. A. *Adv. Mater.* **2001**, *13*, 1501−1505.

(9) Jana, N. R.; Gearheart, L.; Murphy, C. J. *Langmuir* **2001**, *17*, 6782−6786.

(10) (a) Yu, Y. Y.; Chang, S. S.; Lee, C. L.; Wang, C. R. C. *J. Phys. Chem. B* **1997**, *101*, 6661−6664. (b) Gao, J. C.; Bender, M.; Murphy, C. J. *Langmuir* **2003**, *19*, 9065−9070. (c) Gai, P. L.; Harmer, M. A. *Nano Lett.* **2002**, *2*, 771−774. (d) Niidome, Y.; Nishioka, K.; Kawasaki, H.; Yamada, S. *Chem. Commun.* **2003**, 2376−2377.

(11) (a) Shao, Y.; Jin, Y.; Dong, S. *Chem. Commun.* **2004**, 1104−1105. (b) Malikova, N.; Pastoriza-Santos, I.; Schierhorn, M.; Kotov, N. A.; Liz-Marzan, L. M. *Langmuir* **2002**, *18*, 3694−3697. (c) Sarma, T. K.; Chattopadhyay, A. *Langmuir* **2004**, *20*, 3520−3524.

10.1021/cm048292g CCC: $30.25
Published on Web 01/14/2005

Oldenburg et al. have shown that the absorption in the NIR may be tuned in $Au-SiO_2$ core−shell nanostructures by varying the thickness of the gold shell[12]—these core−shell nanoparticles are currently being investigated for commercial application in cancer hyperthermia.[13] Gold nanotriangles with large NIR absorption could be a very effective and a convenient substitute for such core−shell nanoparitcles not involving any cumbersome preparation methods. The NIR absorption of the gold nanotriangles would also be important in architectural applications such as heat-absorbing optical coatings for windows in countries with abundant solar energy.[14] NIR reflective coatings for windows are currently employed and nanomaterials with NIR-absorbing characteristics could provide an attractive alternative to cutting down NIR transmission through windows in buildings.[14]

In this paper, we present a detailed study of the synthesis of gold nanotriangles by the reaction of lemongrass extract with aqueous gold ions. The emphasis is on controlling the size of the gold nanotriangles by varying the experimental conditions in the synthesis and thereby modulate the optical properties of the nanotriangles. We show that size control can be achieved by simple variation in the concentration of the lemongrass extract in the reaction medium and that the longitudinal SPR band in NIR region can be easily tuned. We also present the first results on application of films of the nanotriangles on glass in NIR-absorbing coatings. In a simple experiment, we show that the presence of gold nanotriangle-coated glass placed before an IR source results in a 5 °C reduction in temperature on the other side of the glass window. Presented below are details of the investigation.

Experimental Section

A 100-g aliquot of thoroughly washed lemongrass leaves was finely cut and boiled in 100 mL of sterile distilled water. A 0.1−1.9-mL aliquot of this leaf extract was added to 5 mL of 10^{-3} M aqueous $HAuCl_4$ solution separately, and the volume was made up to 7 mL with addition of appropriate amount of water. UV−visible−NIR spectra were recorded after allowing the reaction medium to stand for 48 h when reduction of Au^{3+} ions in all the reaction mixtures had reached saturation. UV−visible−NIR spectroscopy measurements were carried out on a Jasco dual-beam spectrophotometer (model V-570) operated at a resolution of 1 nm. Transmission electron microscopy (TEM) measurements of the gold nanoparticles synthesized using lemongrass extract were carried out on a JEOL model 1200EX instrument operated at an accelerating voltage at 80 kV. Samples for the TEM were prepared by drop-coating the carbon-coated copper grids placed on a clean Teflon piece with aqueous gold nanoparticle solution. Samples of lemongrass-reduced gold nanotriangles prepared by solution-casting onto highly oriented pyrolytic graphite (HOPG) substrate were analyzed by atomic force microscopy (AFM) in the contact mode on a VEECO Digital Instruments multimode scanning probe microscope equipped with a Nanoscope IV controller. High-resolution transmission electron microscopy (HRTEM) of the samples prepared on carbon-coated grids were carried on a JEOL model 3010 operated at an accelerating voltage of 300 kV. X-ray photoelectron spectroscopy (XPS) analysis of the sodium borohydride reduced spherical gold nanoparticles and lemongrass-reduced gold nanoparticle films deposited on Si (111) wafers were carried out on a VG MicroTech ESCA 3000 instrument at a pressure better than 1×10^{-9} Torr. The general scan and C 1s and Au 4f core level spectra were recorded with un-monochromatized Mg Kα radiation (photon energy, 1253.6 eV) at a pass energy of 50 eV and electron takeoff angle (angle between electron emission direction and surface plane) of 60°. The overall resolution of measurement is thus ~1 eV for the XPS measurements. The core level spectra were background corrected using the Shirley algorithm and the chemically distinct species resolved using a nonlinear least squares procedure. The core level binding energies (BEs) were aligned with the adventitious carbon binding energy of 285 eV.

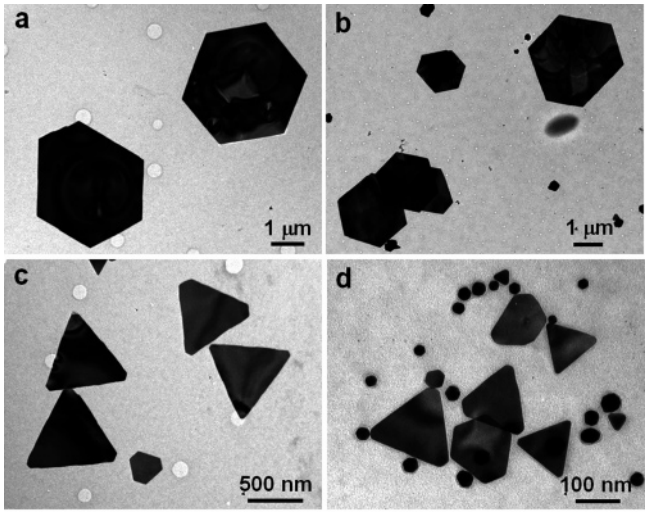

Figure 1. Representative TEM images of gold nanoparticles synthesized by the reduction of 5 mL of 10^{-3} M aqueous $HAuCl_4$ solution with (a) 0.2, (b) 0.3, (c) 0.5, and (d) 1.0 mL of lemon grass extract.

Study of the cooling effect due to infrared absorption in gold nanotriangle-coated glass in comparison with uncoated glass was done by measuring the variation in temperature as a function of time within an enclosed box of cardboard of dimensions 20 cm × 10 cm × 10 cm with a window opening of dimensions, 2 cm × 2.5 cm covered with (a) uncoated glass, (b) glass coated with spherical gold nanoparticle (7.3 mg/cm^2), (c) single layer of gold nanotriangle (4.4 mg/cm^2), (d) three layers of gold nanotriangle-coated glass (13.3 mg/cm^2), and (e) the three-layer gold nanotriangle film after heating at 300 °C for 3 h. The box fitted with required glass sample was irradiated with a 250-W tungsten filament IR lamp kept at a distance of 20 cm from the box.

Results and Discussion

Figure 1 shows representative TEM images of gold nanoparticles synthesized by the reaction of aqueous $AuCl_4^-$ ions by different amounts of lemongrass extract after 48 h of reaction. It is observed that with increasing amount of extract added to the $HAuCl_4$, solution the average size of the triangular and hexagonal particles decreases. Another observation is that the ratio of the number of spherical nanoparticles to triangular/hexagonal particles increases with increasing amount of lemongrass extract in the reaction

(12) Oldenburg, S. J.; Jackson, J. B.; Westcott, S. L.; Halas, N. J. *Appl. Phys. Lett.* **1999**, *75*, 2897−2895.
(13) (a) Loo, C.; Lin, A.; Hirsch, L.; Lee, M. H.; Barton, J.; Halas, N.; West, J.; Drezek, R. *Technol. Cancer Res. Treat.* **2004**, *3*, 33−40. (b) Hirsch, L. R.; Stafford, R. J.; Bankson, J. A.; Sershen, S. R.; Rivera, B.; Price, R. E.; Hazle, J. D.; Halas, N. J.; West, J. L. *Proc. Natl. Acad. Sci. U.S.A.* **2003**, *100*, 1354913554. (c) Nanospectra biosciences, Inc., Huston, TX, www.nanospectra.com.
(14) Xu, X.; Stevens, M.; Cortie, M. B. *Chem Mater.* **2004**, *16*, 2259−2266.

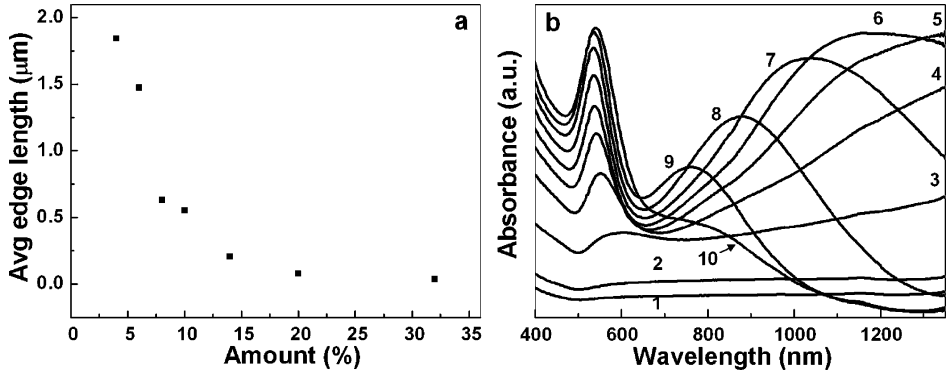

Figure 2. (a) Average edge length variation in gold nanotriangles and truncated triangles as a function of volume percentage of lemongrass extract in 10^{-3} M $HAuCl_4$ solution. (b) UV−visible−NIR spectra of gold nanoparticles synthesized by adding different amount of lemongrass leaf extract to 5 mL of 10^{-3} M $HAuCl_4$ solution. Curves 1−10 correspond to solutions with 0.2, 0.3, 0.4, 0.5, 0.6, 0.7, 0.8, 1.0, 1.2, and 1.6 mL of lemongrass leaf extract in 5 mL of 10^{-3} M $HAuCl_4$ solution, respectively.

medium (compare, for example, Figure 1a and Figure 1d). Figure 2a shows a plot of the average edge length of the triangular and hexagonal gold nanoparticles formed as a function of volume percentage of lemon grass extract added to the 10^{-3} M $HAuCl_4$ solution. The triangular and hexagonal particles formed in each case are not monodisperse and show a large spread in the edge lengths. However, the average edge length determined from 100 triangular/hexagonal particles in each reaction does show a correlation with the amount of reducing agent (lemongrass extract) in the reaction medium (Figure 2a)—the edge length decreases monotonically with increasing amount of lemongrass.

Further evidence for the lemongrass concentration dependent variation in the triangle sizes is provided by UV−visible−NIR spectroscopic analysis of the different solutions (Figure 2b). Two important observations are made from these spectra. The first is that as the amount of lemongrass extract in the reaction medium increases, the SPR band centered at 525 nm increases in intensity and indicates an increase in the number of spherical nanoparticles in the reaction medium. This is borne out by the TEM results (Figure 1d) where a large percentage of small spherical gold nanoparticles are seen to coexist with triangular and hexagonally shaped nanoparticles. The second is that this increase in the SPR band intensity at 525 nm is accompanied by a shift to smaller wavelengths of the longitudinal SPR component that appears in the NIR region (Figure 2b). As mentioned briefly earlier, the presence of the longer wavelength component in the UV−visible−NIR spectra is a clear indication of considerable anisotropy in the nanoparticles, a result that is consistent with TEM analysis of the particles that showed triangular/hexagonal particles of high density. The shift to longer wavelengths with reducing amount of lemongrass extract in the reaction medium is also consistent with TEM analysis of the particles that showed an increase in the average edge length of the anisotropic particles (Figure 1 and Figure 2a). Thus, it is possible to vary the edge length of gold nanotriangles synthesized by simple variation of the amount of reducing agent (lemongrass extract) in the reaction medium. The consequent variation in nanoparticle aspect ratio results in the ability to tune the wavelength of absorption in the NIR with important implications in optical coating technology and hyperthermia of cancer cells. In such applications, tuning of the NIR absorption band in the gold nanoparticles is important since they need to be selectively excited without exciting other tissue cells.[15] We would like to mention here that in the reactions involving low concentrations of lemongrass extract in solution (0.2 and 0.3 mL of lemongrass extract), the edge lengths of the gold nanotriangles were large (1.8 ± 0.4 μm and 1.5 ± 0.6 μm, respectively), and the particles settled with time at the bottom of the test tube as a golden colored precipitate. Ultrasonication of this precipitate resulted in reasonably stable dispersions in water as well as organic solvents such as chloroform and toluene thereby leading to the possibility of forming films of the nanotriangles on different substrates.

Figure 3 shows TEM images of single gold nanotriangles/hexagonal particles and the corresponding electron diffraction patterns of particles obtained under conditions of low lemongrass concentration in the reaction medium (0.2 and 0.3 mL of lemongrass extract). In the former case (Figure 3a and b), the triangular and hexagonal particles were single crystalline fcc structured and [111] oriented as observed from the diffraction pattern in Figure 3a.[7,16] In the latter case too (Figure 3c and d), a single crystalline diffraction pattern is observed but most of the triangular and hexagonal gold particles also show additional diffraction spots around the direct beam and around the spots corresponding to {200} and {422} set of planes as shown in Figure 3b. Due to the weak intensity of the diffraction spots corresponding to the 1/3{422} planes, similar hexagonal pattern of spots could not be confirmed around them. Pileni et al. have carried out a detailed analysis of chemically grown silver nanotriangles and observed that the fcc forbidden 1/3{422} reflections occur due to the presence of (111) stacking fault(s) lying parallel to the (111) surface and extending across the entire planar particle.[16] At lower concentration of lemongrass extract in solution (0.2 mL), the degree of truncation of the triangular particles was observed to be higher with more hexagonal particles in solution (Figure 3e). The electron diffraction pattern of the hexagonal gold nanoparticle shown in Figure 3e is represented in Figure 3f. The diffraction

(15) (a) Simpson, C. R.; Kohl, M.; Essenpreis, M.; Cope, M. *Phys. Med. Biol.* **1998**, *43*, 2465−2478. (b) Anderson, R. R.; Parrish, J. A. *J. Invest. Dermatol.* **1981**, *77*, 13−19.
(16) Germain, V.; Li, J.; Ingert, D.; Wang, Z. L.; Pileni, M. P. *J. Phys. Chem. B* **2003**, *107*, 8717−8720.

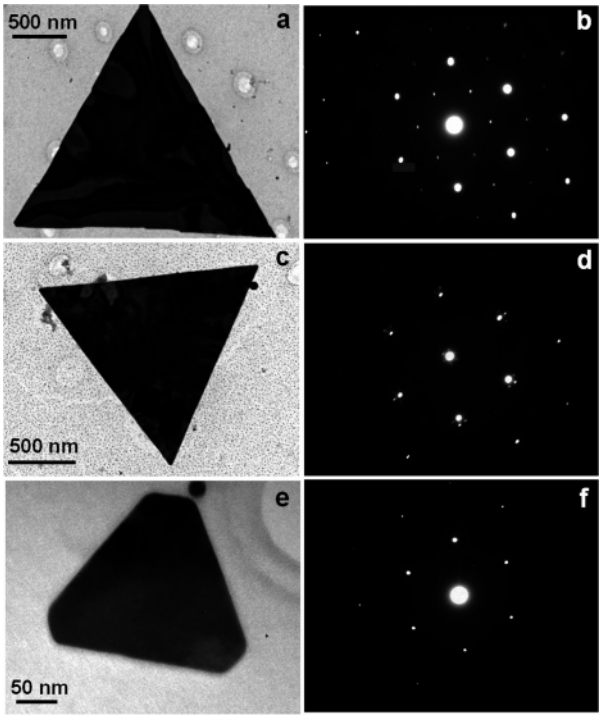

Figure 3. TEM images and the corresponding electron diffraction patterns of gold nanotriangles and hexagons formed on addition of (a, b) 0.2, (c, d) 0.3, and (e, f) 1.0 mL of lemongrass leaf extract to 5 mL of 10^{-3} M $HAuCl_4$ solutions, respectively.

pattern is similar to that obtained for the triangular nanoparticles and indicates ⟨111⟩-orientation of the single crystals.[16] When the added amount of lemongrass extract exceeds 0.7 mL per 5 mL of 10^{-3} M $HAuCl_4$, the stable gold nanoparticle solution obtained consists only of a small fraction of triangular and hexagonal nanoparticles, the major fraction being spherical. We have also observed that the time taken for completion of reaction reduces progressively from 32 to 3 h as the concentration of lemongrass extract in solution increases from 0.2 to 1.6 mL in the reaction medium. This may be rationalized on the basis of two models. The first is based on the formation of spherical "seeds" that then act as centers around which nanotriangle growth occurs through the interaction of shape-directing molecules present in solution. Such a mechanism has been invoked by Mirkin et al. in their study on the growth of silver nanoprisms by a photoirradiation process.[17] For such a process to occur in this study, the rate of formation of spherical nuclei should be slow enough to enable deposition of gold in the form of triangles around the spheres and would clearly be facilitated under conditions of low lemongrass concentration in solution as observed. The second possible model could be one in which the rate of creation of spherical gold nanoparticles competes with assembly and sintering of the particles to triangular/hexagonal structures. At this stage we are unable to comment on the likely mechanism leading to lemongrass mediated formation of gold nanotriangles and further work is in progress to resolve this issue.

A representative AFM micrograph of a gold nanotriangle obtained by reacting 0.4 mL of lemongrass extract with 5 mL of 10^{-3} M aqueous $HAuCl_4$ solution is shown in Figure 4a (top image). The truncation of edges in the triangle is clearly evident in the AFM image. This is a feature repeatedly seen for a large fraction of the nanotriangles obtained (Figure 1). Indeed, such truncated nanotriangles have also been observed for silver[16,17] and gold nanostructures[11] obtained by chemical methods. It is not clear at this stage what the forces are that drive the formation of such structures. A topographic height analysis along the triangle along the direction indicated by the black line in the image is shown in the bottom part of Figure 4a. It is seen that the particle has a height of ∼25 nm and is quite smooth over the surface. The electron diffraction analysis of the nanotriangles (Figure 3) indicated that they were ⟨111⟩-oriented. The line profile analysis of the nanotriangle indicates that the crystal planes bounding the edges of the triangle are not perpendicular to the (111) plane bounding the surface of the nanotriangle. Figure 4b shows the HRTEM image of the vertex of one of the hexagons. The lattice spacing for the observed lattice planes is ∼2.39 Å and is parallel to one of the edges of the hexagonal gold nanoparticle. The observed *d* spacing for these lattice planes does not correspond to the forbidden 1/3(422) reflection plane reported earlier for triangular silver nanoparticles.[16] At this stage, we are unable to assign Miller indices to this set of lattice planes.

A chemical analysis of lemongrass-reduced gold nanoparticles was carried out by X-ray photoemission spectroscopy (XPS) and compared with that of nanoparticles obtained by standard sodium borohydride reduction of aqueous chloroauric acid.[18] Panels a and b in Figure 5 show the C 1s and Au 4f core levels, respectively, for sodium borohydride reduced gold nanoparticles. The C 1s core level has only one chemically distinct component centered at 285 eV binding energy (BE) and is due to adventitious carbon in the sample (Figure 5a). The Au $4f_{7/2}$ core level could be decomposed into two chemically distinct components centered at 83.6 and 85.5 eV BEs that correspond to Au(0) and Au(I) respectively (Figure 5b). The relatively small amount of Au(I) present on the surface of the gold nanoparticles is responsible for the high BE peak and is believed to stabilize the particles electrostatically against aggregation in solution.[18] In the case of lemongrass-reduced gold nanotriangles and hexagons, the C 1s photoemission spectrum is more complex and could be decomposed into four chemically distinct components (Figure 5c). In addition to the adventitious C 1s peak at 285 eV BE, peaks at 282.2, 286.6, and 288.7 eV BE are observed. The low BE peak at 282.2 eV is attributed to aromatic carbons of biomolecules bound to the surface of the gold nanotriangles. The high BE peak at 288.7 eV BE is attributed to electron emission from carbons in carbonyl groups (aldehydic or ketonic carbons),[19] while the peak at 286.6 eV BE is most likely from carbons α to the carbonyl carbons. Induction effects are known to influence the BEs of carbons complexed with electron withdrawing functional groups such as carbonyls.[20] It is also possible that

(17) Jin, R.; Cao, Y.; Mirkin, C. A.; Kelly, K. L.; Schatz, G. C.; Zheng, J. G. *Science* **2001**, *294*, 1901−1903.
(18) Liu, Y. C.; Chuang, T. C. *J. Phys. Chem. B* **2003**, *107*, 12383−12386.
(19) (a) Miyama, T.; Yonezawa, Y. *Langmuir* **2004**, *20*, 5918−5923. (b) Kumar, A.; Mandal, S.; Selvakannan, P. R.; Pasricha, R.; Mandale, A. B.; Sastry, M. *Langmuir* **2003**, *19*, 6277−6282.
(20) Sastry, M.; Ganguly, P. *J. Phys. Chem. A* **1998**, *102*, 697−702.

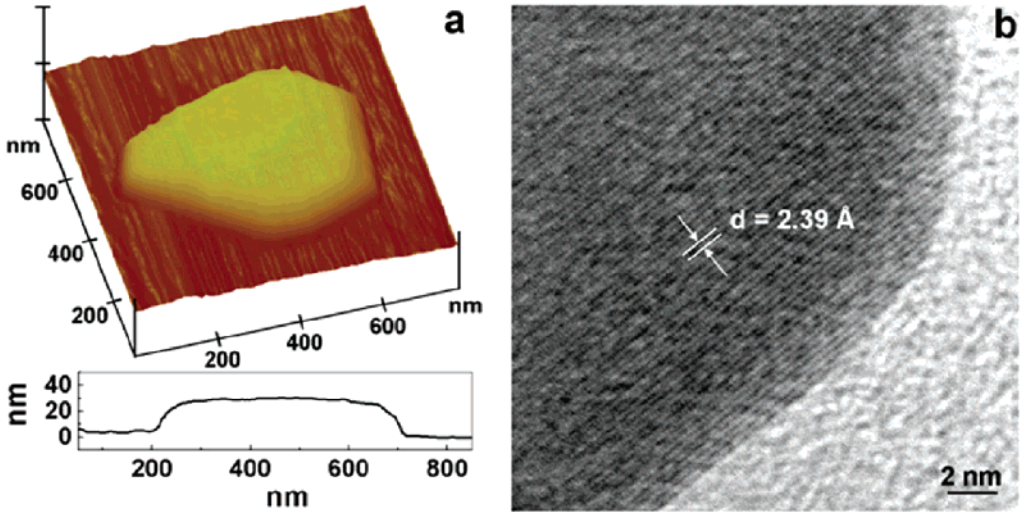

Figure 4. (a) AFM image of one of the truncated triangles formed by reduction of Au^{3+} ions using lemongrass leaf extract. The bottom plot represents topographic height analysis of the triangle along the line marked in the AFM micrograph. (b) HRTEM image from the vertex of one of the hexagonal gold nanoparticles.

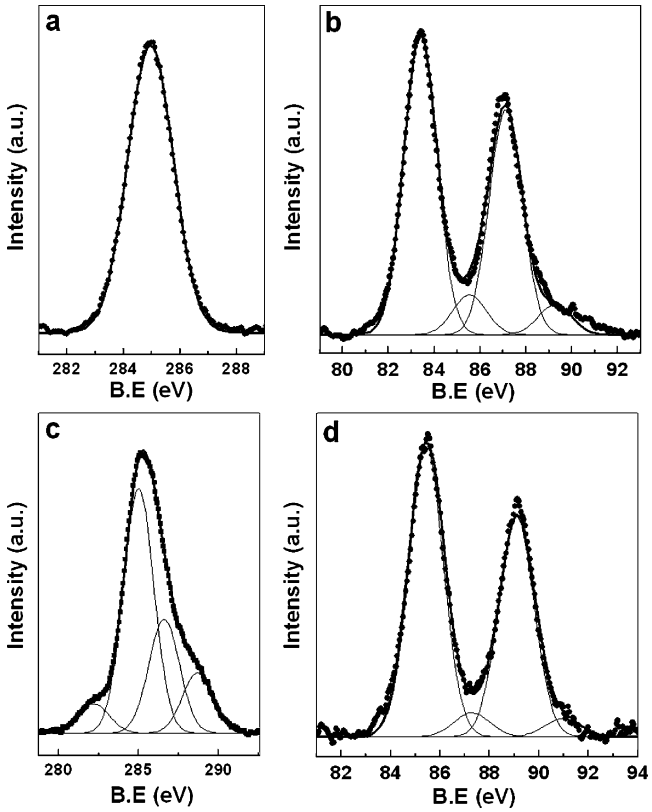

Figure 5. (a, b) XPS C1s and Au 4f core level spectra, respectively, recorded from sodium borohydride reduced gold nanoparticles. (c, d) XPS C 1s and Au 4f core level, respectively, from lemongrass leaf extract reduced gold nanoparticles.

this peak in the C 1s spectrum could arise from carbons coordinated to hydroxyl groups in sugar derivatives present in the lemongrass leaf extract and complexed with the gold nanotriangles. The sugar derivative molecules through the carbonyl groups are believed to direct the assembly of the initially formed small spherical gold nanoparticles (less than 3 nm diameter) as discussed in our previous report.[7] In a recent report, it has been shown that assembly and sintering of gold nanoparticles could promote the formation of gold nanocubes at elevated temperatures.[21]

The energy in the solar spectrum is primarily centered around the visible and infrared region of the electromagnetic spectrum.[22] For architectural constructions in high temperature geographical locations, it is required for glass coatings to be optically transparent but infrared opaque. Such coatings reduce the temperature rise within enclosed rooms, thus considerably reducing power expenditure on cooling of interiors. This may be accomplished by designing coatings that either reflect[23] or absorb IR radiation. In current architectural applications, the former approach is preferred. The possibility of tuning the longitudinal SPR absorption band over a wide range of wavelengths from ~700 nm to well into the NIR region of the electromagnetic spectrum for the anisotropic triangular and hexagonal gold nanoparticles make them well suited for architectural applications[14,23] and cancer hyperthermia.[13] We show below through a simple experiment that glass coatings with IR absorbing elements such as those provided by our lemongrass extract synthesized gold nanotriangles could provide an interesting alternative. In this experiment, the temperature rise within a cardboard box with an aperture to fix various glass substrates due to exposure to an infrared lamp was recorded as a function of time of exposure. Curves 1 and 2 in Figure 6a correspond to the UV−visible−NIR transmission spectra recorded from a glass substrate coated with three layers of gold nanotriangles obtained in the 0.2-mL lemongrass reaction medium before and after heating at 300 °C for 3 h. In the case of the as-prepared coating, the transmission in the NIR region is quite low due to absorption by the nanotriangles (curve 1). After heat treatment of the film, the transmission in the NIR increases (curve 2) indicating some sintering of the nanotriangles and loss in their anisotropic structure. The as-deposited gold nanotriangle film has a pretty bluish color

(21) Jin, R.; Egusa, S.; Scherer, N. F. *J. Am. Chem. Soc.* **2004**, *126*, 9900−9901.
(22) ASTMG 159−98. Standard tables for references solar spectral irradiance at air mass 1.5: Direct normal and hemispherical for a 37° tilted surface; American Society for Testing and Materials: West Conshohocken, PA, 1998.
(23) (a) Arnaud, A. *J. Non-Cryst. Solids* **1997**, *218*, 12−18. (b) Manning, T. D.; Parkin, I. P. *J. Mater. Chem.* **2004**, *14*, 2554−2559.

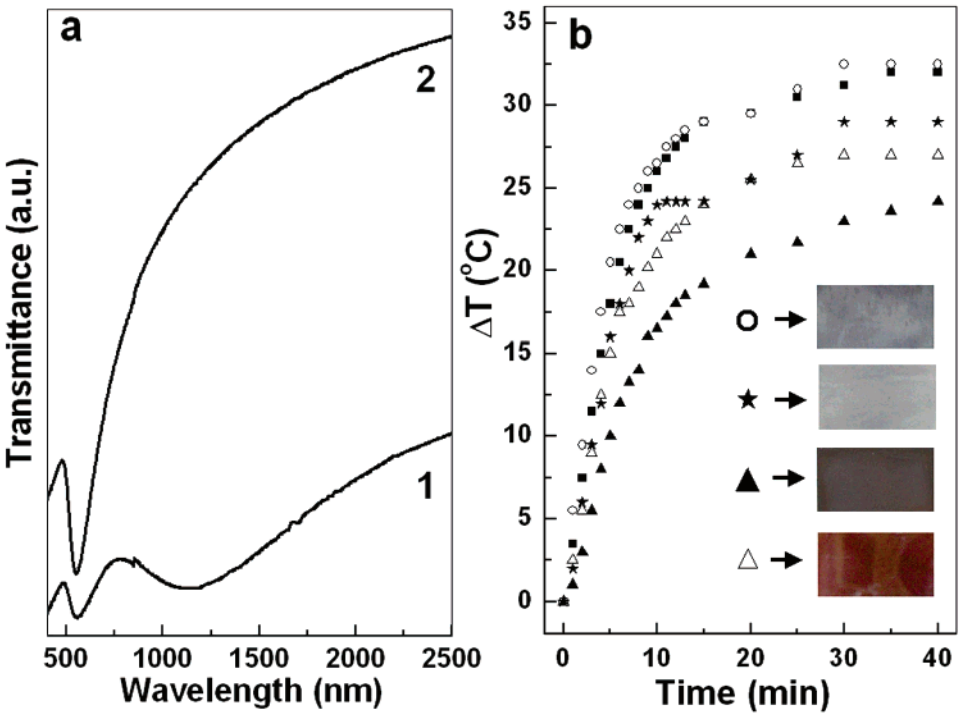

Figure 6. (a) UV−visible−NIR transmission spectra of lemongrass-reduced gold nanotriangles. Curve 1: film of gold nanotriangles spray-coated onto glass substrate maintained at 80 °C. Curve 2: after heat treatment of the above film at 300 °C for 3 h. (b) Temperature difference (with respect to ambient temperature, 28 °C) vs time measured inside a thermally insulated box exposed to an IR lamp with a window blocked with uncoated glass (squares); glass coated with spherical gold nanoparticles (open circles); glass coated with one layer of lemongrass extract prepared gold nanotriangles (stars) and three layers of gold nanotriangles (solid triangles); and the three-layer gold nanotriangle sample after heat treatment (open triangles). The inset shows photographs of the different glass samples with coatings identified by the corresponding symbols.

(inset of Figure 6b, photograph corresponding to filled triangles) and could thus serve dual purposes of providing tinted glass (indeed, the color of the coating could be varied from light pink to blue to dark gray) and an IR absorbing coating. After heat treatment, the film color turned to a golden hue (inset of Figure 6b, photo corresponding to open triangles) and despite the increased IR transmission, was still effective in blocking IR radiation (vide infra).

Figure 6b shows plots of the variation of temperature within an enclosed box of cardboard with an window covered with (a) uncoated glass (squares) and glass coated with (b) spherical, borohydride reduced gold nanoparticles (7.3 mg/cm^2, circles), (c) a single layer of gold nanotriangles (4.4 mg/cm^2, stars), (d) three layers of gold nanotriangles (13.4 mg/cm^2, solid triangles), and (e) three layers of gold nanotriangles after heating at 300 °C for 3 h (open triangles) as a function of time of exposure to an IR lamp positioned at a distance of 20 cm from the window. It is observed that after irradiation with a tungsten filament lamp using either uncoated glass (squares) or the glass coated with spherical gold nanoparticles (open circles) as a window, the temperature rise follows a similar trend and that the temperature within the enclosure increases by 32 °C relative to the ambient room temperature (28 °C) within 30 min of exposure. Thus, spherical gold nanoparticles do not lead to a drop in temperature within the enclosure, a result consistent with the fact that spherical gold nanoparticles do not absorb in the NIR region. In the case of the glass coated with one layer of gold nanotriangles (stars), the temperature rise within the enclosure could be brought down to 27 °C while on using the glass coated with three layers of gold nanotriangles (solid triangles), the difference in temperature with respect to the ambient temperature could be brought down to as low as 23 °C. This drastic reduction in temperature due to infrared blocking by the gold nanotriangle film on the glass can clearly lead to a huge savings in the expenditure required to cool interiors of structures in geographically hot locations. To test the role of heat treatment of the film on the infrared absorbing capability of the nanotriangle coatings, the three-layer nanotriangle film on glass was heated at 300 °C for 3 h in air. On using the heat-treated gold nanotriangle coated glass as a window, we observe that the temperature rise inside the enclosure has now increased to 26 °C (open triangles). Thus, there is a small loss in IR absorbing efficiency of the gold nanotriangle coating after this heat treatment and is consistent with the increased IR transmission measured for this film (Figure 6a, curve 2). After this heat treatment, it was observed that the color of the film changed to a golden hue (when viewed at slightly off normal) and that the color was more uniform over the surface. Even after this heat treatment, it is seen that the film is still capable of blocking out a considerable amount of IR radiation (compare with behavior of plain glass, squares). Since the synthesis of triangular and hexagonal gold particles used in the coatings is a solution method employing plant extract based reducing agents, we believe it would be an economically viable approach to forming infrared-absorbing thin coatings on different surfaces.

Conclusions

We have shown that by simple variation in the experimental conditions, it is possible to tune the size of gold nanotriangles synthesized by the reaction of lemongrass extract with aqueous gold ions. This results in an easy method for modulating the optical properties of the nanotriangles, particularly the near-infrared absorption behavior of the nanoparticles. The NIR absorption of the gold nanotriangles has important implications in hyperthermia of cancer cells as well as IR-blockers in optical coatings for architectural applications. We have shown that films of the nanotriangles of varying thickness can be readily cast on glass substrates and that these films are efficient absorbers of IR radiation in an application where the temperature in a compartment exposed to an infrared source was considerably reduced by the presence of the nanotriangle coating on a glass window.

Acknowledgment. S.S.S. and A.R. thank the Council of Scientific and Industrial Research (CSIR), Government of India, for financial assistance. We gratefully acknowledge Ms. Renu Pasricha for TEM measurements, Ms. Meenakshi Chaudhary for the AFM measurements, and Ms. Usha Govind Tumkur from JNCASR Bangalore for HRTEM measurements.

CM048292G